Neurobiology of Aging 78 (2019) 18–28

Contents lists available at ScienceDirect

Neurobiology of Aging

journal homepage: www.elsevier.com/locate/neuaging

Lentiviral vector–mediated overexpression of Klotho in the brain improves Alzheimer's disease–like pathology and cognitive deficits in mice

Chen-Ye Zeng [a,1], Ting-Ting Yang [a,1], Hong-Jing Zhou [a,1], Yue Zhao [a], Xi Kuang [a], Wei Duan [b], Jun-Rong Du [a,*]

[a] Department of Pharmacology, Key Laboratory of Drug-Targeting and Drug Delivery System of the Education Ministry, Sichuan Engineering Laboratory for Plant-Sourced Drug and Sichuan Research Center for Drug Precision Industrial Technology, West China School of Pharmacy, Sichuan University, Chengdu, China
[b] School of Medicine and Centre for Molecular and Medical Research, Deakin University, Waurn Ponds, Victoria, Australia

ARTICLE INFO

Article history:
Received 8 October 2018
Received in revised form 25 January 2019
Accepted 2 February 2019
Available online 13 February 2019

Keywords:
Alzheimer's disease
Klotho
Cognitive function
Amyloid beta
Autophagy
Microglia

ABSTRACT

Alzheimer's disease (AD) is the most common type of senile dementia. The antiaging gene *Klotho* is reported to decline in the brain of patients and animals with AD. However, the role of *Klotho* in the progression of AD remains elusive. The present study explored the effects and underlying mechanism of *Klotho* in a mouse model of AD. The upregulation of cerebral *Klotho* expression was mediated by an intracerebroventricular injection of a lentiviral vector that encoded *Klotho* (LV-KL) in 7-month-old amyloid precursor protein/presenilin 1 transgenic mice. Three months later, LV-KL significantly induced *Klotho* overexpression in the brain and effectively ameliorated cognitive deficit and AD-like pathology in amyloid precursor protein/presenilin 1 mice. LV-KL induced autophagy activation and protein kinase B/mammalian target of rapamycin inhibition both in AD mice and BV2 murine microglia. These results suggest that the upregulation of *Klotho* expression in the brain may promote the autophagic clearance of amyloid beta and protect against cognitive deficits in AD mice. These findings highlight the preventive and therapeutic potential of *Klotho* for the treatment of AD.

1. Introduction

Alzheimer's disease (AD) is an age-related polygenetic neurodegenerative disorder that is characterized by progressive cognitive decline. No effective therapies for AD have yet been developed (Kalaria et al., 2008; Mayeux et al., 2012). The amyloid beta (Aβ) cascade hypothesis has been used to explain the main pathogenesis of AD for the past 20 years (Hardy et al., 1992; Murphy et al., 2010). Recently, BAN2401 (an anti-Aβ protofibril antibody) and the anti-amyloid agent GV-971 successfully passed phase II/III clinical trials for the treatment of AD (Cummings et al., 2018). These findings provide convincing evidence to support the amyloid hypothesis, indicating that the search for approaches to lower Aβ through accelerated clearance or inhibition of its production may be a novel therapeutic strategy for the treatment of AD.

Aβ is generated by the sequential proteolytic cleavage of amyloid precursor protein (APP), resulting in the formation of 40- to 42 amino acid peptides (Mandrekar et al., 2010). In the healthy brain, soluble Aβ enters extracellular fluid and can be effectively cleared (Roberts et al., 2014; Wang et al., 2006). However, in the brains of patients with AD, the overaccumulation of soluble peptides that is induced by Aβ overproduction or impairments in its clearance spontaneously aggregates to form Aβ oligomers and fibrils, which are subsequently deposited to form diffuse and dense core amyloid plaques (Mandrekar et al., 2010). Studies have shown that impairment in Aβ clearance rather than the overproduction of Aβ is the central event in AD. Aβ clearance rates decreased in patients with AD, and Aβ production rates might remain unchanged compared with healthy individuals (Jiang et al., 2014; Mawuenyega et al., 2010). Autophagy is an important pathway for clearing Aβ aggregates. Autophagy has been reported to be markedly impaired in patients and animals with AD (Jiang et al., 2014; Lee et al., 2014; Roberts et al., 2014), suggesting that the dysfunction of autophagy may play an important role in the development of Aβ pathology.

The antiaging gene *Klotho* is predominantly located in the kidney and choroid plexus and may encode membrane-anchored and secreted isoforms (sKL) through alternative RNA splicing (Bloch

* Corresponding author at: Department of Pharmacology, Sichuan University, Chengdu 610041, China. Tel.: +86 28 85503938; fax: +86 28 85501371.
E-mail address: dujr_1@163.com (J.-R. Du).
[1] These three authors contributed equally to this work.

0197-4580/$ – see front matter © 2019 Elsevier Inc. All rights reserved.
https://doi.org/10.1016/j.neurobiolaging.2019.02.003

et al., 2009; Kuro-o et al., 1997; Kurosu et al., 2005). The single-pass transmembrane *Klotho* can be shed by secretases, and the cleaved ectodomain (cKL) is secreted into the blood and cerebrospinal fluid (Bloch et al., 2009; Chen et al., 2007). Both sKL and cKL are referred to as soluble Klotho and may act as a multiple functional antiaging hormone (Cararo-Lopes et al., 2017; Masso et al., 2017). Studies showed that elderly individuals with AD had lower Klotho concentrations in cerebrospinal fluid compared with elderly individuals without AD, and the expression of Klotho in brain areas decayed more rapidly in various mouse models of AD such as human APP (hAPP), APP/presenilin 1 (PS1), and 3 × Tg AD transgenic mice compared with wild-type (WT) controls (Dubal et al., 2015; Kuang et al., 2017; Masso et al., 2015; Semba et al., 2014). Hemizygous hAPP mice crossed with hemizygous Klotho (KL) transgenic mice produced the transgenic hAPP/KL mice, which had elevated Klotho expression and enhanced cognition (Dubal et al., 2015). Our previous study found that ligustilide, a natural Klotho enhancer, might ameliorate AD-like pathology and cognitive impairments in APP/PS1 mice (Kuang et al., 2017). Notably, Bian reported that the Klotho-induced upregulation of autophagy flux might contribute to Klotho-mediated renoprotection (Bian et al., 2015). Autophagy is known to be negatively regulated by the phosphorylation of mammalian target of rapamycin (mTOR) (Wang et al., 2015). Phosphoinositide 3-kinase/protein kinase B (AKT) is one of the upstream kinases that may regulate mTOR signaling (Cai et al., 2012). Studies have shown that *Klotho* may inhibit the insulin/insulin-like growth factor-1/Phosphoinositide 3-kinase/AKT signaling cascade in the aging process (Kurosu et al., 2005). We also found that *Klotho* ablation that was induced by *Klotho* siRNA could stimulate insulin-like growth factor-1/AKT/mTOR signaling in vitro (Kuang et al., 2017). Based on accumulating evidence, we hypothesized that *Klotho* might exert AD-modifying effects through the induction of autophagy-induced Aβ clearance. In the present study, we induced *Klotho* overexpression using a lentivirus that encoded the transmembrane form of mouse *Klotho* (LV-KL) in the brain in APP/PS1 mice and cultured murine microglia, and investigated the effects of LV-KL on AD and the underlying mechanism.

2. Materials and methods

The main contents of this section are presented in Supplementary Information.

2.1. Animals

Male 6.5-month-old $APP^{swe}/PS1^{dE9}$ (line 85) (referred to as APP/PS1) transgenic mice that harbored mutant mouse/human APP (Swedish K595N/M596L) and PS1 genes (PS1-dE9) were purchased from Beijing HFK Bioscience Co, Ltd (Beijing, China) (Jankowsky et al., 2004). Age-matched nontransgenic mice that had the same genetic background (C57BL/6J) as APP/PS1 mice were used as normal controls (referred to as WT). The animals were housed at 22 °C ± 2 °C under a 12 h/12 hours light/dark cycle with free access to food and water. The animal studies were conducted in accordance with the Regulations of Experimental Animal Administration issued by the State Committee of Science and Technology of China. All the animal procedures were approved by the Animal Research Committee of the West China School of Pharmacy, Sichuan University.

2.2. Lentiviral vector preparation and intracerebroventricular administration

The lentiviral vector that encoded the transmembrane full-length form of mouse *Klotho* cDNA (LV-KL) and control lentiviral vector that encoded green florescence protein (LV-GFP) were obtained from OriGene Technologies (Rockville, MD, USA). The lentiviral vectors were prepared as we previously reported (Zhou et al., 2017). The lentiviral titer was measured by flow cytometry as described in Supplement Information (Fig. S1). After 2 weeks of acclimatization, thirty 7-month-old APP/PS1 mice were randomly divided into 2 groups: APP/PS1/LV-GFP and APP/PS1/LV-KL ($n = 15$ per group), and received a bilateral i.c.v. injection of LV-KL or LV-GFP (3 μL/side, 2.65×10^7 TU/mL), respectively (Zhou et al., 2017). And 15 age-matched C57BL/6J mice were similarly administrated with LV-GFP (WT group). Two APP/PS1 mice that were treated with LV-GFP died within 2 weeks after lentivirus administration.

2.3. Determination of the uptake and degradation of $A\beta_{1\text{-}42}$ in microglial cells

In the present study, the lentivirus carried a GFP tag, which interferes with observations of FITC signals of FITC-labeled $A\beta_{1\text{-}42}$ fibrils (F-fAβ). Therefore, we tested the effects of the recombinant ectodomain of mouse Klotho (1819-KL-050; R&D Systems, Minneapolis, MN, USA; one of the main functional fragments of cKL) (Chen et al., 2013, 2015; Wu et al., 2013; Zeldich et al., 2014) on the phagocytosis of fibrillary $A\beta_{1\text{-}42}$. The preparation of F-fAβ and culture of BV2 murine microglia are described in Supplementary Information (Fig. S2A). After preincubation with Klotho protein (400 ng/mL) or volume-matched vehicle for 4 hours, the cells (4×10^4/well) were treated with 1 μM F-fAβ or vehicle for the indicated time, followed by incubation with LysoTracker Red (50 nM) and Hoechst 33342 for another 15 minutes. The cells were then washed with -buffered saline (PBS), and images were acquired under a fluorescence microscope (Nikon, Tokyo, Japan).

2.4. In vitro viral transduction and $A\beta_{1\text{-}42}$ treatment in microglial cells

BV2 cells (2×10^5/well) were incubated for 5 hours, and 75 μL of PBS, LV-KL, or LV-GFP (2.65×10^7 TU/mL) was added to the culture medium with polybrene (8 μg/mL). Forty-eight hours later, the cells were harvested for the determination of *Klotho* mRNA levels by real-time polymerase chain reaction (Zhou et al., 2018). Seventy-two hours later, cell transfection efficiency was digitized using a 10× objective under a microscope, and Klotho protein levels in cell pellets and the supernatant were measured by Western blot and enzyme-linked immunosorbent assay, respectively (Kuang et al., 2017; Zhou et al., 2017).

To detect the effect of *Klotho* on the autophagy-mediated clearance of fibrillary $A\beta_{1\text{-}42}$ (fAβ) in vitro, the cells were treated with fresh culture medium with and without 1 μM fAβ (Fig. S4B) for another 2 hours. After 72 hours of virus transfection, the cells were washed with PBS and collected to determine the expression of effectors of autophagy. The specific AKT agonist SC-79 (B5663, APExBIO, Taiwan, China) was added to a final concentration of 4 μg/mL only 1 hour before the addition of fAβ, and the same volume of PBS was added to the untreated group.

2.5. Statistical analysis

SPSS 19.0 software was used for the statistical analyses. Correlational analysis was performed using Spearman rank-order correlation. The remaining data were analyzed by one-way analysis of variance with Dunnett's test. Values of $p < 0.05$ were considered statistically significant.

3. Results

3.1. Klotho overexpression ameliorated cognitive deficits in APP/PS1 mice

Three months after i.c.v. administration of the lentivirus (Fig. 1A and B), we examined Klotho expression in the brain. As shown in Fig. 1C and D, Klotho mRNA and protein levels significantly decreased by 46% and 54%, respectively, in the choroid plexus in 10-month-old APP/PS1/LV-GFP mice compared with the age-matched WT/LV-GFP group, respectively ($p < 0.01$). LV-KL significantly upregulated Klotho mRNA and protein levels in the choroid plexus in APP/PS1 mice compared with APP/PS1/LV-GFP controls ($p < 0.01$). Moreover, a ~50% decrease in Klotho mRNA levels was found in brain tissues in APP/PS1/LV-GFP mice compared with the age-matched WT/LV-GFP group ($p < 0.01$; Fig. 1E), and this decrease was significantly reversed by LV-KL ($p < 0.05$). Consistent with previous results in aged mice (Zhou et al., 2017), LV-KL significantly restored *Klotho* expression in the choroid plexus and brain in AD mice.

Three neurobehavioral tests were then performed to evaluate cognitive function. Short-term and long-term working memory abilities were evaluated in the Y-maze and passive avoidance test. As shown in Fig. 1F, a significant difference in alternation performance was observed among groups in the Y-maze ($F_{2,40} = 50.181$, $p < 0.001$). Specifically, the percentage of alternation in the WT/LV-GFP group was 68.8% ± 2.2%, whereas the percentage of alternation in APP/PS1/LV-GFP mice decreased to 42.5% ± 2.9% ($p < 0.01$). Treatment with LV-KL significantly increased alternation performance in AD mice to 67.2% ± 3.1% compared with the APP/PS1/LV-GFP group ($p < 0.01$). In the passive avoidance test (Fig. 1G), we observed a significant decrease in step-down latency (107 ± 25 seconds) and a significant increase in the number of step-down errors (1.61 ± 0.21) in the APP/PS1/LV-GFP group compared with WT/LV-GFP controls (227 ± 26 seconds and 0.53 ± 0.16, respectively, $p < 0.01$), and these effects were significantly reversed by LV-KL (225 ± 27 seconds and 0.67 ± 0.23, $p < 0.01$, vs. APP/PS1/LV-GFP group). The Morris water maze test was performed to examine the effect of LV-KL on spatial learning and memory ability in AD mice (Fig. 1H and I). In the hidden platform test, APP/PS1/LV-GFP mice exhibited a significantly longer escape latency compared with WT/LV-GFP controls ($p < 0.01$), which was significantly shortened by LV-KL treatment ($p < 0.01$, vs. APP/PS1/LV-GFP). In the space exploration test, the number of platform crossings (0.61 ± 0.18) and percent time in the target quadrant (22.7% ± 2.4%) significantly decreased in the APP/PS1/LV-GFP group compared with WT/LV-GFP mice (3.40 ± 0.25 and 39.1% ± 2.5%, respectively, $p < 0.01$). Notably, LV-KL effectively improved these behavioral deficits in AD mice compared with APP/PS1/LV-GFP controls, reflected by an increase in the number of platform crossings (1.4 ± 0.21) and increase in the percent time in the target quadrant (31.7% ± 3.2%, $p < 0.05$). These results suggest that Klotho overexpression may improve cognitive deficits in AD mice. In contrast to the cognitive improvement induced by LV-KL in AD mice, LV-KL did not significantly affect the neurobehavioral performances in WT mice in the 3 tests (our unpublished data).

3.2. Klotho overexpression reduced Aβ deposits in APP/PS1 mice

Congo red staining and $A\beta_{1\text{-}42}$ immunostaining were used to detect compact amyloid plaques and $A\beta_{1\text{-}42}$-positive amyloid plaques in the brain. As shown in Fig. 2A and B, no amyloid plaques were detected in the brain in WT/LV-GFP mice, whereas Aβ plaque accumulation was observed in the cortex and hippocampus in APP/PS1/LV-GFP mice. In contrast, LV-KL induced an approximately 50% reduction of total amyloid plaques in both the cortex and hippocampus in AD mice ($p < 0.05$ and 0.01, vs. APP/PS1/LV-GFP group; Fig. 2A and B). We performed enzyme-linked immunosorbent assay to quantify the levels of $A\beta_{1\text{-}42}$ and $A\beta_{1\text{-}40}$ in the brain. As shown in Fig. 2C, the levels of soluble and insoluble $A\beta_{1\text{-}42}$ (316 ± 25 pg/mg and 539 ± 48 pg/mg, respectively) in the brain in the APP/PS1/LV-GFP group were significantly higher than in the WT/LV-GFP group (123 ± 19 pg/mg and 240 ± 33 pg/mg, respectively; $p < 0.01$). Moderate increases in the levels of soluble and insoluble $A\beta_{1\text{-}40}$ were observed in the brain in APP/PS1/LV-GFP mice compared with the WT/LV-GFP group ($p < 0.05$; Fig. 2C). Remarkably, LV-KL significantly decreased the levels of both soluble and insoluble $A\beta_{1\text{-}42}$ and $A\beta_{1\text{-}40}$ in the brain in AD mice compared with APP/PS1/LV-GFP controls ($p < 0.05$ and 0.01; Fig. 2C). The current findings are inconsistent with what Dubal et al. previously observed in hAPP/KL transgenic mice, in which knock-in *Klotho* reduced cognitive decline without altering the Aβ level in the hippocampus (Dubal et al., 2015).

Some observations showed that a failure of the clearance of excessive Aβ from the brain may lead to cerebral amyloid angiopathy (CAA) (Preston et al., 2003). Therefore, Congo red staining and laminin immunostaining were used to detect the possible effects of *Klotho* on vascular Aβ deposition in APP/PS1 mice. No detectable vascular amyloid deposition was observed in WT/LV-GFP mice. However, LV-KL induced a 48% decrease in entire cortical CAA in LV-KL–treated APP/PS1 mice (0.062% ± 0.006%) compared with LV-GFP–treated AD controls (0.12% ± 0.014%; $p < 0.01$; Fig. 2D and E).

3.3. Klotho overexpression ameliorated neurovascular unit damage in APP/PS1 mice

Cerebral amyloidosis may cause neurovascular unit damage and thus promote the progression of AD. Therefore, we first investigated the effects of *Klotho* on the extent of neuronal loss in the brain in AD mice. Three months after LV-GFP transduction, Nissl staining and NeuN immunostaining revealed ~40% neuronal loss in the cerebral cortex in 10-month-old APP/PS1 mice compared with WT mice ($p < 0.01$; Fig. 3A and B). Consistent with a previous study (Barbero-Camps et al., 2013), no significant neuronal loss was observed in the hippocampal cornu ammonis (CA1) area in 10-month-old AD mice compared with WT controls ($p > 0.05$; Fig. S3), which was likely attributable to fewer Aβ plaques in the hippocampus (Fig. 2A and B). LV-KL significantly preserved neuronal survival in the cortex in APP/PS1 mice ($p < 0.01$, vs. APP/PS1/GFP group; Fig. 3A and B). Early synaptic deficits may precede neuronal loss in APP/PS1 mice (Barbero-Camps et al., 2013). Therefore, we examined the expression of synaptophysin, an integral membrane protein of small synaptic vesicles. As shown in Fig. 3A and C, immunostaining revealed ~40% reductions of synaptophysin expression in the hippocampus and cortex in APP/PS1/LV-GFP mice compared with WT/LV-GFP controls ($p < 0.01$), which was significantly rescued by LV-KL ($p < 0.01$). Moreover, Western blot confirmed the protective effect of LV-KL on synaptophysin expression in the brain in APP/PS1 mice compared with LV-GFP–treated AD mice ($p < 0.05$; Fig. 3D and E). In addition, the accumulation of Aβ aggregates may promote the phosphorylation of tau (p-tau), resulting in the formation of neurofibrillary tangles. In the present study, we observed a 2-fold increase in the level of p-tau in the brain in APP/PS1/LV-GFP mice compared with the WT/LV-GFP group, and LV-KL induced a 24% reduction of p-tau in AD mice ($p < 0.01$, vs. APP/PS1/LV-GFP group; Fig. 3F).

Brain pericytes are one of the major elements of the neurovascular unit, playing an important role in the progression of AD through the regulation of blood-brain barrier integrity and brain capillary perfusion (Sagare et al., 2013). We examined vascular

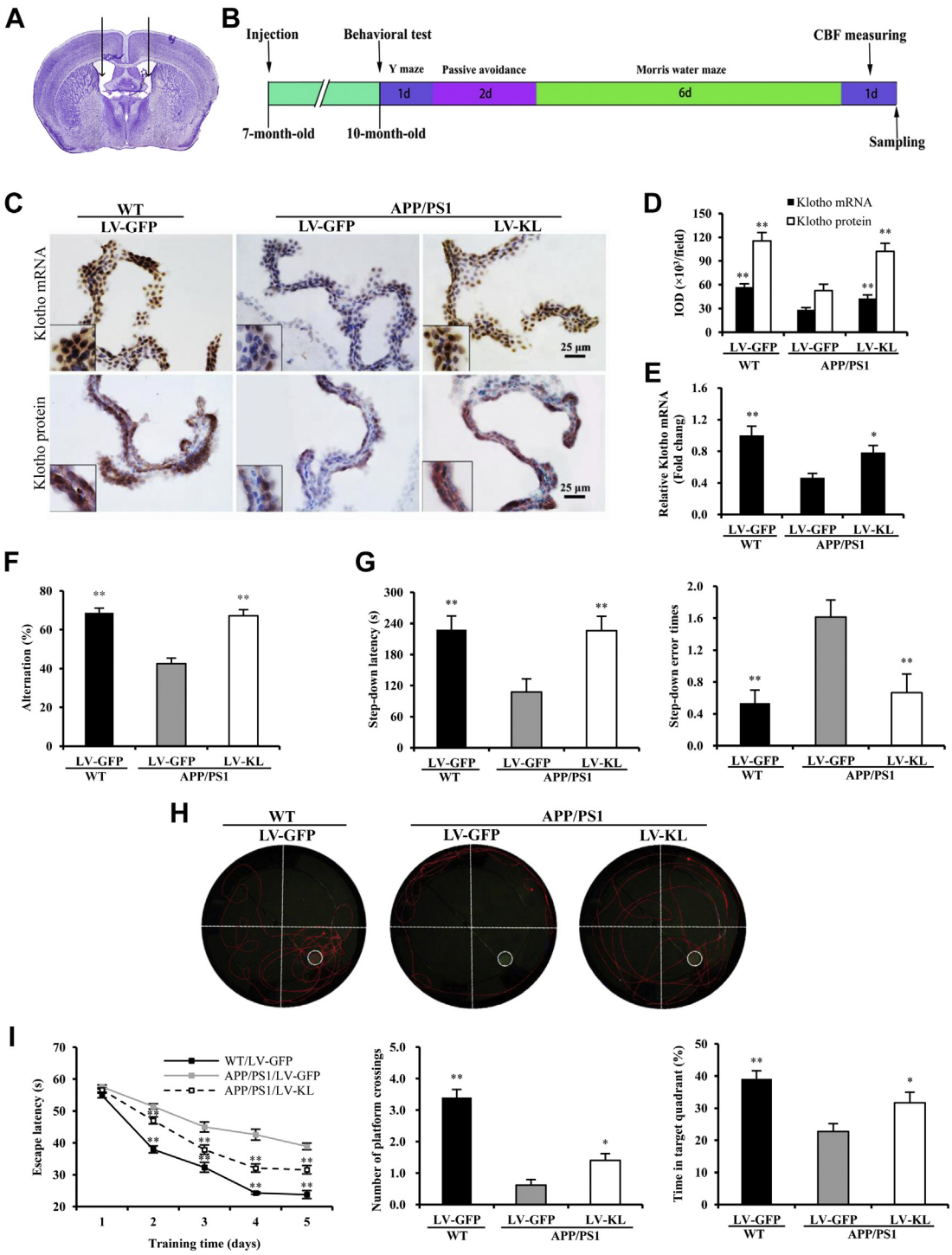

Fig. 1. LV-KL–induced intracerebral Klotho overexpression and improved cognitive deficits in amyloid precursor protein/presenilin 1 (APP/PS1) mice. Seven-month-old APP/PS1 and wild-type (WT) mice were intracerebroventricularly administered a lentivirus that encoded *Klotho* (LV-KL) or green fluorescent protein (LV-GFP) and were sacrificed at 10 months of age for analysis. (A) Lateral ventricular injection sites of lentivirus in mouse brain. (B) Time course of the experiment. (C) In situ hybridization assay of *Klotho* mRNA levels and immunohistochemistry of Klotho protein levels in the choroid plexus in the brain. The inset shows representative overall staining intensity. (D) Quantitative image analysis of *Klotho* mRNA levels and protein expression based on the integrated optical density (IOD) of positive immunostaining (brown). (E) PCR analysis of *Klotho* mRNA levels in brain tissues. The relative mRNA levels of Klotho were normalized to GAPDH and are expressed as fold induction relative to the LV-GFP–treated WT group. (F) Percentage of alternation in the Y-maze. (G) Step-down latency and number of errors in the passive avoidance test. (H) Characteristic swimming trails in the probe test of the Morris water maze. (I) Escape latency, number of platform crossings, and percent time in the target quadrant in the Morris water maze. $n = 10–12$/group for histological staining (C–E). $n = 13–15$/group for neurobehavioral tests (F–I). The data are expressed mean ± SEM. $^{*}p < 0.05$, $^{**}p < 0.01$, versus APP/PS1/LV-GFP group (one-way ANOVA followed by Dunnett's test). (For interpretation of the references to color in this figure legend, the reader is referred to the Web version of this article.)

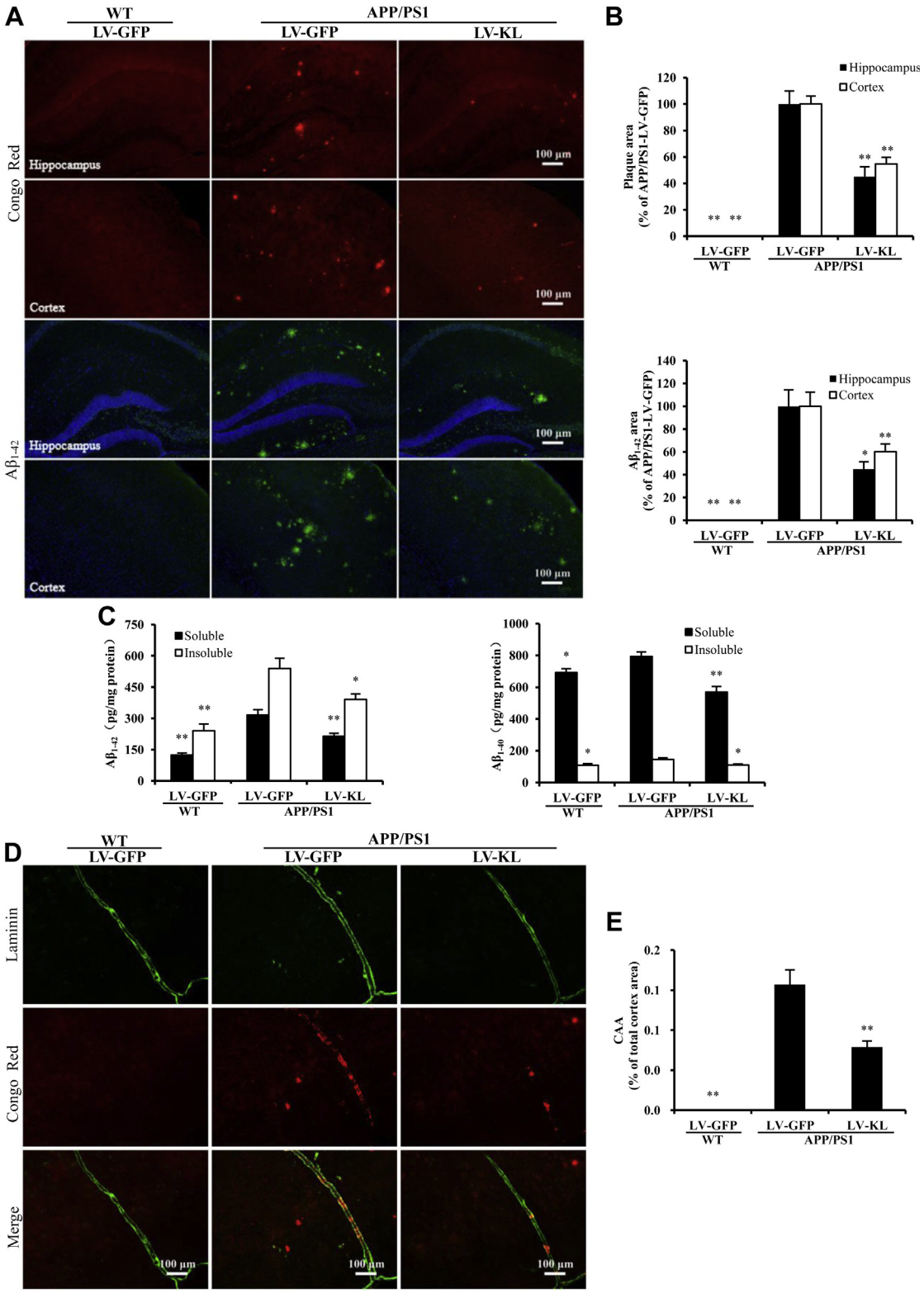

Fig. 2. LV-KL decreased Aβ burden in APP/PS1 mice. Three months after lentivirus administration, the brain was collected from 10-month-old mice to determine Aβ burden in vivo. (A and B) Representative images and quantitative analysis of Aβ plaques by Congo red staining and $A\beta_{1\text{-}42}$ immunostaining in the hippocampus and cerebral cortex. $n = 10–12$/group. (C) $A\beta_{1\text{-}42}$ and $A\beta_{1\text{-}40}$ levels in the brain were measured by ELISA. $n = 6$/group. (D and E) Representative images of cerebral amyloid angiopathy (CAA), revealed by Congo red staining and Laminin immunostaining, and quantitative analysis of the percentage of CAA area in the total cerebral cortex area. $n = 6$/group. The data are expressed as mean ± SEM. $^{*}p < 0.05$, $^{**}p < 0.01$, versus APP/PS1 group treated with LV-GFP (one-way ANOVA followed by Dunnett's test). Abbreviations: LV-KL, lentiviral vector that encoded *Klotho*; LV-GFP, lentivirus that encoded green fluorescent protein; APP/PS1, amyloid precursor protein/presenilin 1; Aβ, amyloid beta; ELISA, enzyme-linked immunosorbent assay. (For interpretation of the references to color in this figure legend, the reader is referred to the Web version of this article.)

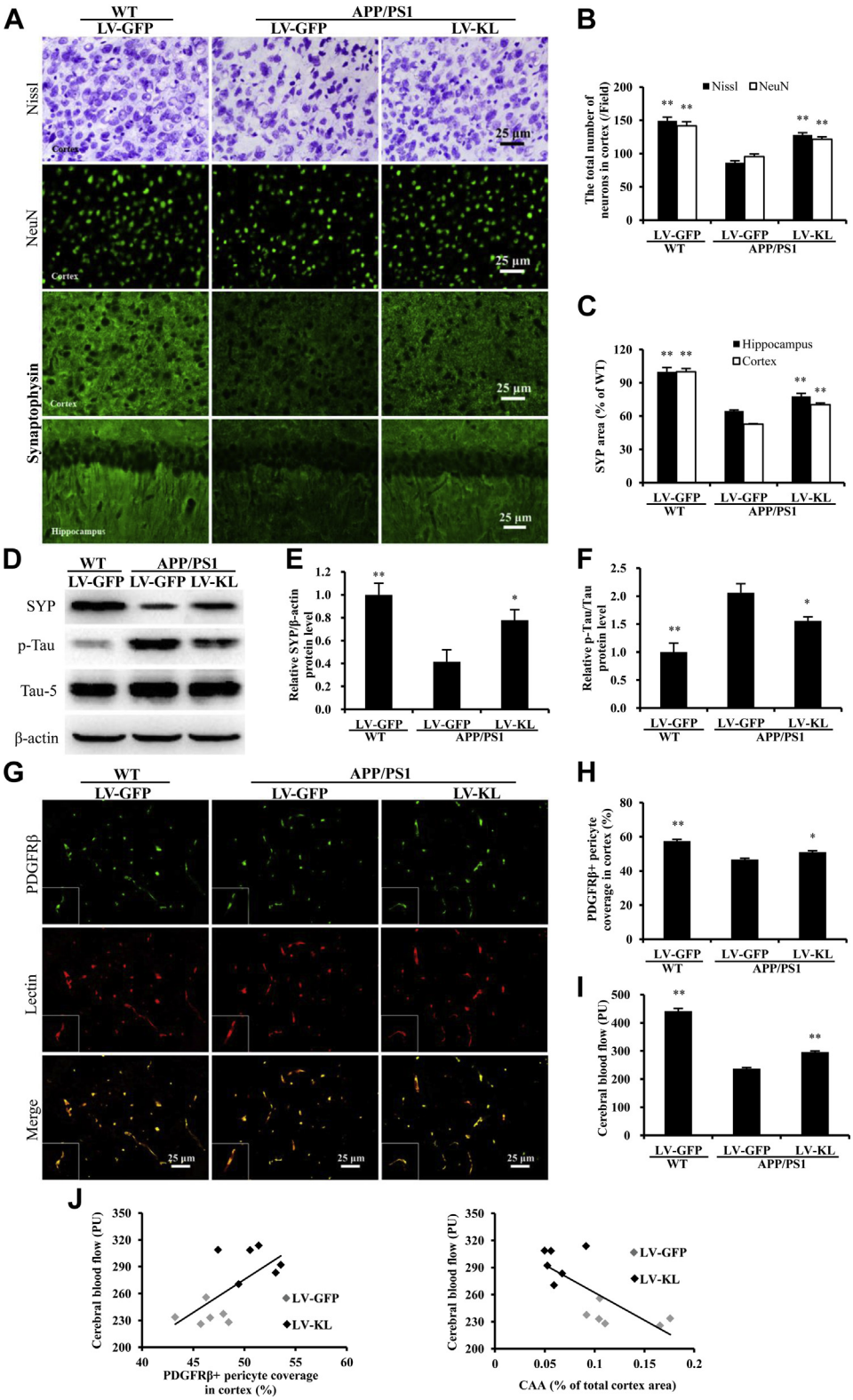

Fig. 3. LV-KL ameliorated neurovascular injury in APP/PS1 mice. Three months after lentivirus transduction, the brain was collected from 10-month-old mice to examine AD-like neurovascular injury. (A) Representative images of neuron and synaptophysin (SYP), analyzed by histological staining, in the cortex and hippocampus. (B and C) Quantitative analysis of the number of Nissl-positive and NeuN-positive neurons and the synaptophysin-positive area. $n = 8$/group. (D–F) Representative immunoblots and quantitative analysis of SYP expression and tau phosphorylation in brain tissues. The levels of SYP and p-tau were normalized to β-actin and tau-5, respectively. The results are expressed as the normalized optical density value relative to the LV-GFP–treated WT group. $n = 4$/group. (G) Representative images of PDGFR-β–positive pericytes (green) and lectin-positive capillary endothelium (red) in the cortex. (H) Quantitative analysis of the coverage of PDGFR-β–positive pericytes based on the merged positive fluorescent area in the cortex. $n = 6$/group. (I) CBF was detected by laser Doppler perfusion imaging in the cortex. $n = 13$–15/group. (J) Correlation between CBF and vascular PDGFR-β–positive pericyte coverage or CAA area, analyzed by Spearman rank-order correlation ($p < 0.05$). $n = 6$/group. The data are expressed as mean ± SEM. (A–I) $^{*}p < 0.05$, $^{**}p < 0.01$, versus LV-GFP–treated APP/PS1 group (one-way ANOVA followed by Dunnett's test). Abbreviations: AD, Alzheimer's disease; LV-KL, lentiviral vector that encoded *Klotho*; APP/PS1, amyloid precursor protein/presenilin 1; LV-GFP, lentivirus that encoded green fluorescent protein; PDGFR-β, platelet-derived growth factor receptor β; CBF, cerebral blood flow; CAA, cerebral amyloid angiopathy; WT, wild type. (For interpretation of the references to color in this figure legend, the reader is referred to the Web version of this article.)

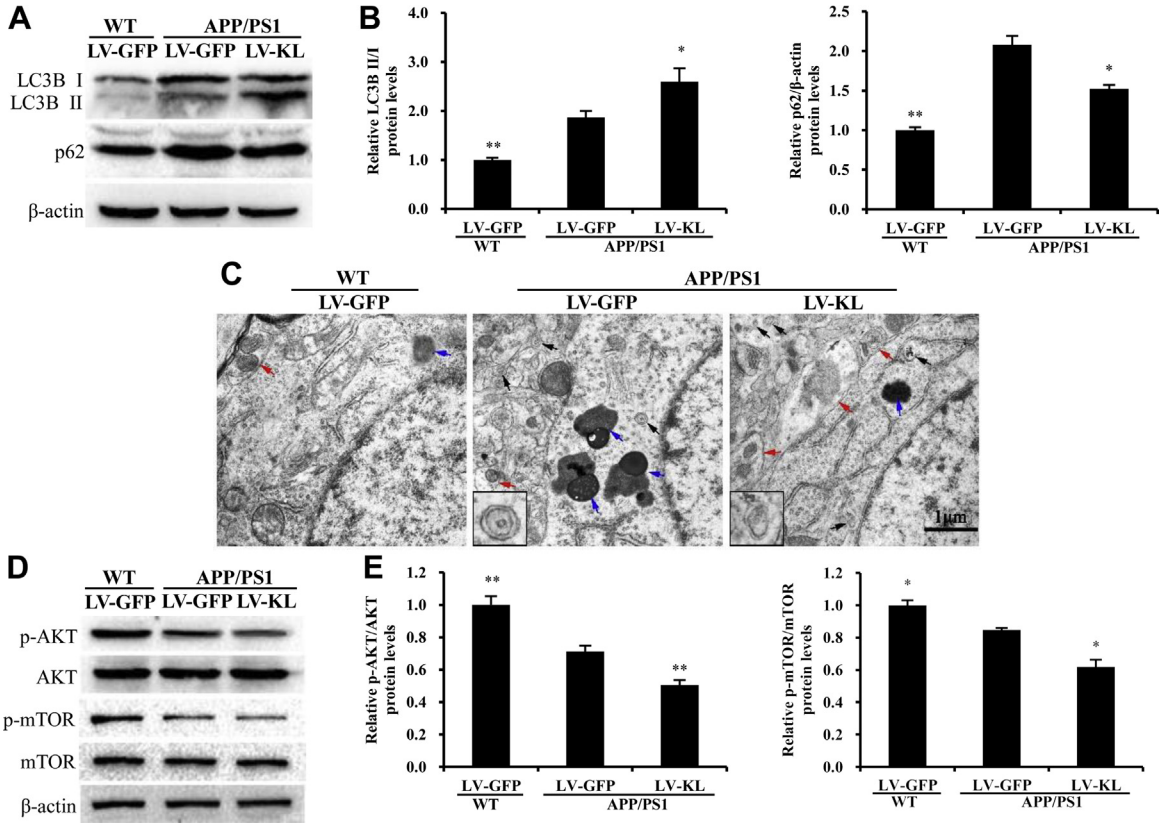

Fig. 4. LV-KL promoted autophagy in the brain in APP/PS1 mice. Three months after lentivirus transduction, the brain was collected from 10-month-old mice for Western blot and transmission electron microscopy. (A and B) Representative immunoblots and quantitative analysis of autophagy markers. The expression levels of LC3B II and *p*62 were normalized to LC3B I and β-actin, respectively. The data were normalized to the LV-GFP–treated WT group. $n = 4$/group. (C) Transmission electron microscope sections from the cortex. The black arrows indicate autophagosomes. The red arrows indicate autolysosomes. The blue arrows indicate lipofuscin. $n = 3$/group. (D and E) Representative immunoblots and quantitative analysis of phosphorylation of AKT (p-AKT) and mTOR (p-mTOR). For Western blot, the expression levels of LC3B II, *p*62, p-AKT, and p-mTOR were normalized to LC3B I, β-actin, AKT, and mTOR, respectively. The data were normalized to the LV-GFP–treated WT group. $n = 4$/group. The data are expressed as mean ± SEM. $^{*}p < 0.05$, $^{**}p < 0.01$, versus LV-GFP–treated APP/PS1 group (one-way ANOVA followed by Dunnett's test). Abbreviations: LV-KL, lentiviral vector that encoded *Klotho*; APP/PS1, amyloid precursor protein/presenilin 1; LV-GFP, lentivirus that encoded green fluorescent protein; WT, wild type; mTOR, mammalian target of rapamycin; AKT, protein kinase B. (For interpretation of the references to color in this figure legend, the reader is referred to the Web version of this article.)

pericyte coverage by immunostaining with platelet-derived growth factor receptor β (a marker of pericytes) and *Lycopersicon esculentum* (tomato) lectin (a marker of endothelial cells) and measured cerebral blood flow (CBF) in the mouse cerebral cortex. Three months after the i.c.v. injection of LV-GFP, APP/PS1 mice exhibited significant decreases in pericyte coverage and CBF in the cortex compared with WT mice ($p < 0.01$; Fig. 3G–I). Notably, LV-KL significantly increased vascular pericyte coverage and CBF in the cortex in APP/PS1 mice compared with LV-GFP–treated APP/PS1 controls ($p < 0.05$ and 0.01). Furthermore, the correlational analysis showed that cortical CBF was positively correlated with the rate of vascular pericyte coverage ($r = 0.66$, $p < 0.05$; Fig. 3J) and negatively correlated with the extent of CAA ($r = 0.74$, $p < 0.05$; Fig. 3J), suggesting that the protective effects of *Klotho* against brain capillary dysfunction are likely attributable to the attenuation of both pericyte degradation and vascular amyloid deposition in AD mice.

3.4. *Klotho* overexpression induced autophagy in the brain in APP/PS1 mice

To explore the potential mechanism by which *Klotho* overexpression significantly reduced Aβ deposits in AD mice, we examined the expression of autophagy-related proteins, autophagosome-associated light chain 3B (LC3B) and *p*62, in the brain (Fig. 4A and B). Three months after LV-GFP administration, APP/PS1/LV-GFP mice exhibited a ~86% increase in the LC3B II-to-LC3B I ratio and a 2-fold increase in *p*62 levels in the brain compared with WT controls ($p < 0.01$), indicating an increase in autophagy dysfunction in the brain in AD animals. Interestingly, LV-KL induced a 39% increase in the LC3B II-to-LC3B I ratio and a 26% decrease in *p*62 levels in the brain in APP/PS1 mice ($p < 0.05$, vs. APP/PS1/LV-GFP), suggesting an improvement of autophagy in LV-KL–treated AD mice. The changes in autophagy in the cortex were further confirmed by transmission electron microscopy (Fig. 4C). Consistent with the changes in markers of autophagy, an increase in the accumulation of autophagosomes (black arrows) was observed in APP/PS1/LV-GFP mice compared with WT/LV-GFP controls, whereas LV-KL significantly increased autolysosomes (red arrows) in AD mice. We also detected lipofuscin deposition (blue arrows) in the cortex in LV-GFP–treated AD mice, which was significantly reduced by LV-KL treatment. Furthermore, Western blot showed that LV-KL significantly inhibited the phosphorylation of AKT and mTOR in the brain in AD mice compared with the APP/PS1/LV-GFP group ($p < 0.05$ and 0.01; Fig. 4D and E). These results suggest that the upregulation of *Klotho* expression might promote the autophagy-lysosome system and improve autophagic function in AD mice, which was associated with the inhibition of mTOR signaling.

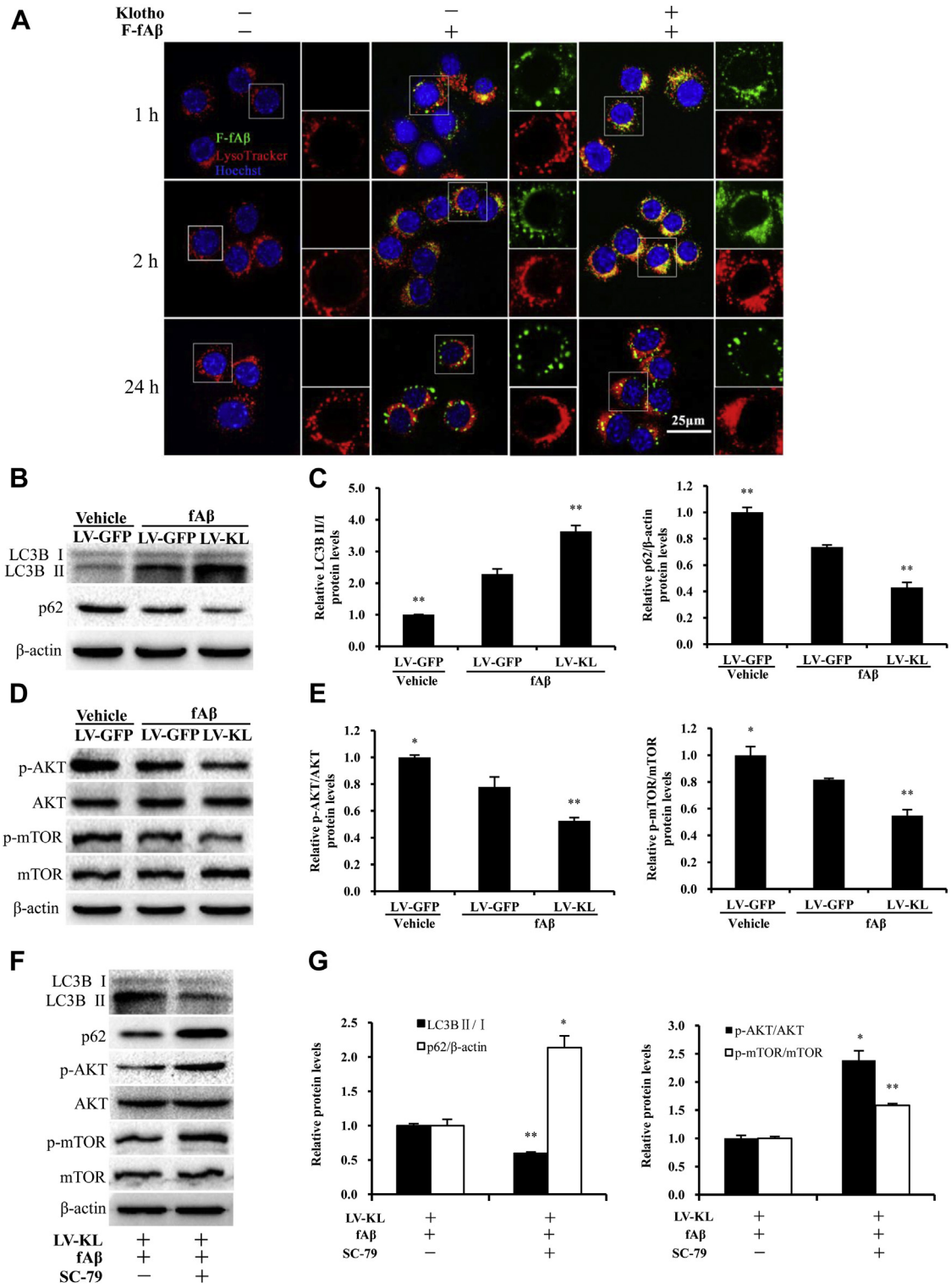

Fig. 5. LV-KL stimulated autophagic clearance of Aβ1-42 in BV2 cells. (A) Representative images of the microglial phagocytosis of fibrillary $A\beta_{1\text{-}42}$ in vitro. Murine microglial BV2 cells were treated with vehicle or mouse recombinant Klotho protein (400 ng/L) for 4 hours and incubated with dimethyl sulfoxide (DMSO) or 1 μM FITC-labeled $A\beta_{1\text{-}42}$ fibrils (F-fAβ; Fig. S2A) and incubated for the indicated time, followed by staining with LysoTracker Red and Hoechst 33342. (B–E) Representative immunoblots and quantitative analysis of the expression of effectors in cell lysates. The cells were treated with LV-GFP or LV-KL for 72 hours, followed by incubation with vehicle or fibrillary $A\beta_{1\text{-}42}$ (fAβ; 1 μM) for another 2 hours. The expression levels of LC3B II, *p*62, phosphorylated AKT (p-AKT), and phosphorylated mTOR (p-mTOR) were normalized to LC3B I, β-actin, AKT, and mTOR, respectively. The results are expressed as each normalized value relative to the vehicle-treated LV-GFP–infected group. (F and G) Representative immunoblots and quantitative analysis of the expression of effectors in cell lysates as shown in panels C and E. The cells were treated with LV-GFP or LV-KL for 71 hours, followed by PBS or SC-79 (AKT agonist, 4 μg/mL) for 1 hour and fAβ (1 μM) for another 2 hours. The results are expressed as each normalized value relative to the LV-KL–treated (without SC-79) group. $n = 3$/group. The data are representative of 3 independent experiments and are expressed as mean ± SEM. $^{*}p < 0.05$, $^{**}p < 0.01$, versus LV-GFP–treated fAβ group (C and E) or LV-KL–treated (without SC-79) group (G) (one-way ANOVA followed by Dunnett's test). Abbreviations: LV-KL, lentiviral vector that encoded *Klotho*; LV-GFP, lentivirus that encoded green fluorescent protein; mTOR, mammalian target of rapamycin; AKT, protein kinase B; PBS, phosphate-buffered saline. (For interpretation of the references to color in this figure legend, the reader is referred to the Web version of this article.)

3.5. Effects of Klotho on the autophagic clearance of $A\beta_{1\text{-}42}$ in microglial cells

In cultured BV2 murine microglia, we observed the time-related uptake and degradation of extracellular FITC-labeled F-fAβ (Fig. 5A). Soluble Klotho protein significantly increased the amount of $A\beta_{1\text{-}42}$ in LysoTracker Red–positive vesicles compared with vehicle-treated cells after 2 hours of incubation with F-fAβ. Moreover, intracellular $A\beta_{1\text{-}42}$ content was significantly reduced in Klotho-treated cells after 24 hours incubation with F-fAβ compared with 2-h treatment. These results suggest that Klotho may promote phagocytosis and the subsequent lysosomal degradation of F-fAβ in microglia.

To clarify the potential mechanism of *Klotho* in the regulation of $A\beta_{1\text{-}42}$ fibril (fAβ) degradation, we first confirmed the transfection efficacy and expression of the lentiviral vector in vitro (Fig. S4). Western blot analysis was performed to examine the effects of *Klotho* on autophagy in fAβ-treated BV2 cells. As shown in Fig. 5B and C, 72 hours after transfection with LV-GFP, fAβ induced a 2-fold increase in LC3B II levels and 27% decrease in *p*62 levels compared with vehicle-treated controls ($p < 0.01$). LV-KL further significantly induced autophagy activation, reflected by a 36% elevation of the LC3B II-to-LC3B I ratio and a 42% reduction of *p*62 levels compared with fAβ/LV-GFP controls ($p < 0.01$). fAβ/LV-GFP significantly decreased the levels of p-AKT and p-mTOR ($p < 0.05$, vs. vehicle/LV-GFP controls; Fig. 5D and E), which was further downregulated by LV-KL ($p < 0.05$). Remarkably, SC-79 (an AKT-specific agonist) significantly reversed LV-KL–induced AKT/mTOR signaling inhibition and autophagy activation ($p < 0.05$ and 0.01). Collectively, these findings suggest that *Klotho* may increase the autophagic clearance of F-fAβ through the inhibition of AKT/mTOR signaling in microglia.

4. Discussion

AD is the most common type of senile dementia. The previous studies showed that the decline of *Klotho* or different isoforms of Klotho (sKL or cKL) is involved in the progression of AD in patients and various transgenic mouse models of AD, respectively (Kuang et al., 2017; Masso et al., 2015; Semba et al., 2014). In the present study, lentiviral vector–induced upregulation of intracerebral *Klotho* expression had significant disease-modifying effects in 10-month-old APP/PS1 transgenic mice, including lowering of Aβ deposition in brain parenchyma and the cerebrovasculature and improvements in tau phosphorylation, neurovascular unit damage, brain capillary dysfunction, and cognitive deficits. The protective effect of *Klotho* against these AD-like phenotypes was associated with the inhibition of AKT/mTOR signaling and activation of the autophagy-mediated clearance of $A\beta_{1\text{-}42}$ in vivo and in vitro.

Numerous studies over the last 2 decades have demonstrated the neurovascular toxicity of aberrant Aβ deposition in the brain, which may trigger a cascade of pathological events in AD. These secondary pathological events can form vicious cycles themselves and accelerate AD progression (Jiao et al., 2015; Sagare et al., 2013). Mutations of APP and PS1 promote cerebral amyloidosis and subsequent AD-like phenotypes in APP/PS1 mice. Seven-month-old APP/PS1 mice begin to exhibit early symptoms of AD, primarily through the accumulation of Aβ, which progressively worsens with age (Reiserer et al., 2007; Wu et al., 2013). Thus, the present study used 7-month-old APP/PS1 mice to evaluate the preventive and therapeutic potential of *Klotho* in AD. Three months after a bilateral i.c.v. injection of lentiviral vectors, LV-KL significantly increased *Klotho* mRNA and protein levels in the choroid plexus and brain tissue in 10-month-old AD mice compared with age-matched AD mice that were treated with the control lentiviral vector (LV-GFP). Intracerebral *Klotho* overexpression improved neurobehavioral performance in the Y-maze, passive avoidance test, and Morris water maze, indicating that *Klotho* may protect against cognitive decline in AD mice. We also found that *Klotho* overexpression significantly ameliorated AD-like neuropathological alterations, such as Aβ accumulation, neuronal and synaptic injury, and the hyperphosphorylation of tau, which may stimulate the formation of neurofibrillary tangles in the brain. In addition, Aβ deposition in cerebral vessels (CAA) and Aβ vascular toxicity strongly affect brain capillary function and the blood-brain barrier, which can further promote the progression of AD (Sagare et al., 2013; Viswanathan et al., 2011). We found that *Klotho* overexpression significantly decreased CAA and increased vascular pericyte coverage and CBF in the cortex in AD mice, suggesting the protective effect of *Klotho* on cerebrovasculature. Altogether, these results demonstrated that intracerebral *Klotho* overexpression by lentiviral transduction can effectively improve multiple AD-like phenotypes in APP/PS1 mice. Considering the pivotal role of Aβ accumulation in the pathogenesis of this mouse model of AD, we speculate that Aβ might be a potential target for *Klotho* intervention.

Autophagy is an important pathway to maintain homeostasis in the central nervous system by removing senescence-related proteins and damaged organelles (Jiang et al., 2014). Numerous studies have demonstrated that autophagy plays an important role in Aβ homeostasis, and its dysfunction is implicated in the development and progression of AD (Tian et al., 2011; Wolfe et al., 2013). In the present study, we first examined the effect of *Klotho* on 2 markers of autophagy: *p*62 (a substrate for autophagy) and LC3B (a specific protein i.e. involved in the entire autophagy process) in vivo. Transmission electron microscopy was used to detect the autophagy process. Consistent with previous reports, we observed autophagy dysfunction in the brain in 10-month-old AD mice, reflected by an abnormal increase in *p*62 levels, a higher LC3B II-to-LC3B I ratio, and an increase in autophagosomes in the brain compared with age-matched WT controls. And the upregulation of intracerebral *Klotho* expression significantly decreased *p*62 levels and increased the LC3B II-to-LC3B I ratio and both autophagosomes and autolysosomes in AD mice. It is well known that microglia, the resident macrophages in the brain, play an important role in maintaining the central nervous system homeostasis. Studies have showed that microglia may promote the uptake and degradation of Aβ fibrils through the autophagic-lysosomal system (Cho et al., 2014; Gold et al., 2015). Therefore, we further evaluated the effect of the ectodomain form of mouse Klotho on fibrillary $A\beta_{1\text{-}42}$ clearance in BV2 microglial cells by staining with LysoTracker Red (a marker of lysosomes or other lysosome-related vesicles). Our results showed that the soluble Klotho protein enhanced the phagolysosomal degradation of extracellular F-fAβ in microglia. Moreover, *Klotho* overexpression that was induced by LV-KL also significantly decreased *p*62 levels and increased the LC3B II-to-LC3B I ratio in F-fAβ-treated BV2 cells. It has been reported that the mTOR signaling pathway is a key pathway in the regulation of autophagy, and the AKT agonist SC-79 can induce downstream mTOR activation (Li et al., 2015; Wang et al., 2015). The current data showed that *Klotho* overexpression significantly inhibited the phosphorylation of AKT and mTOR in both the brain in AD mice and in $A\beta_{1\text{-}42}$ fibril-treated microglia in vitro. SC-79 also significantly reversed both the inhibitory effect on AKT/mTOR signaling and promoting action on autophagy that is mediated by *Klotho* overexpression in microglia that was treated with F-fAβ. Collectively, these findings suggest that *Klotho* may enhance the autophagy-mediated clearance of F-fAβ through inhibition of the AKT/mTOR signaling pathway. In the present study, we also found that intracerebral *Klotho* overexpression decreased $A\beta_{1\text{-}40}$ content in the brain in AD mice. $A\beta_{1\text{-}40}$ comprises a substantial proportion of Aβ in CAA, which could also

be reduced by *Klotho* overexpression. These results suggest that vascular transporters might be involved in the regulatory action of *Klotho* on Aβ clearance. On the other hand, the production of Aβ is thought to be primarily neuronal (Goedert et al., 1987). Our previous study also showed that klotho enhancer, ligustilide, could significantly decrease the intraneuronal Aβ load in the hippocampal CA1 region of aged mice (Kuang et al., 2014). Therefore, further studies should explore the potential effect and mechanism of *Klotho* on the autophagic clearance of Aβ in neurons.

Unlike our results, transgenic expression (knock-in) of *Klotho* in hAPP mice failed to affect Aβ burden (Dubal et al., 2015). This discrepancy may be due to different models. In the previous study, *Klotho* was upregulated since early development. The chronic long-term exposure to *Klotho* may "desensitize" the system, leading to ineffective regulation of *Klotho* at older age. In our study, *Klotho* was not introduced into APP/PS1 mice until at 7 month, when cerebral Aβ plaques begin to form. This acute upregulation of *Klotho* may exert a much stronger effect on Aβ clearance. The phenomenon that chronic long-term exposure induces a weaker biological effect than acute treatment is also observed in other cases. For example, it has been found that recombinant CCL2 induces a much stronger effect on CCL2 null mutants than WT mice (Yao et al., 2011). Thus, animal models and treatment strategy should be taken into consideration in future studies.

Interestingly, transmission electron microscopy showed that *Klotho* overexpression significantly reduced lipofuscin accumulation in cortical cells in 10-month-old APP/PS1 mice. Two early studies reported an increase in yellow-brown lipofuscin in neuronal cells in patients with AD (Dowson et al., 1992, 1995), but no such preclinical or clinical studies of lipofuscin have been conducted more recently. Lipofuscin is an electron-dense substance that is deposited in senescent cells and cannot be further degraded by lysosomes (Hohn et al., 2013; Terman et al., 1998). The massive accumulation of lipofuscin severely affects the function of nerve cells and leads to apoptosis (Terman et al., 1998). In addition, it is reported that the endogenous Klotho elevation improved cognitive and behavioral abnormalities in hAPP/KL mice compared with hAPP mice through regulation of the GluN2B subunit abundance of NMDAR in postsynaptic densities and NMDAR-dependent long-term potentiation (Dubal et al., 2015). These findings suggest that *Klotho* is likely to prevent against the progression of AD by multiple potential mechanisms. Furthermore, the full length of *Klotho* theoretically increases the expression of all isoforms of Klotho, including the transmembrane form of Klotho, c-KL and s-KL (Wu et al., 2013). This is a dilemma for klotho study largely because of the lack of specific methods to distinguish these different forms of Klotho. In the present study, we observed that i.c.v injection of lentivirus encoding the full length of murine klotho gene (LV-KL) induced increases in the klotho mRNA or/and protein expression in the choroid plexus and brain tissues of mice. LV-KL also upregulated the levels of klotho mRNA and protein in the murine BV2 cells as well as the content of the shed isoform of Klotho in the cultured medium. Meanwhile, both LV-KL and the soluble Klotho (one of isoforms of cKL) could activate autophagy in vivo and in vitro. Therefore, the current information suggests that *Klotho* is a disease-modifying therapeutic target for AD. However, the detailed working mode of different isoforms of Klotho still requires further investigation.

In summary, the present study found that the upregulation of intracerebral *Klotho* improved AD-like cognitive impairments and pathological changes in AD (e.g., Aβ accumulation within brain parenchyma and cerebrovasculature, tau hyperphosphorylation, neurovascular unit damage, and brain capillary dysfunction). The underlying mechanism of *Klotho* against AD appears to be at least partially associated with the promotion of $A\beta_{1-42}$ clearance through inhibition of the AKT/mTOR pathway and subsequent activation of the autophagy-lysosome system. These findings provide direct evidence of the potential of intracerebral *Klotho* for the treatment of AD.

Disclosure

The authors declare no conflict of interest.

Acknowledgements

This work was supported by the National Science Foundation of China (81473219) and partly by targeting drug delivery system of Sichuan Province Youth Science and Technology Innovation Team (2016TD0001), 111 Project of the National Ministry of Education (B18035), and the Open Research Fund of State Key Laboratory Breeding Base of Systematic research, development and Utilization of Chinese Medicine Resources.

Appendix A. Supplementary data

Supplementary data associated with this article can be found, in the online version, at https://doi.org/10.1016/j.neurobiolaging.2019.02.003.

References

Barbero-Camps, E., Fernández, A., Martínez, L., Fernández-Checa, J.C., Colell, A., 2013. APP/PS1 mice overexpressing SREBP-2 exhibit combined Abeta accumulation and tau pathology underlying Alzheimer's disease. Hum. Mol. Genet. 22, 3460–3476.
Bian, A., Neyra, J.A., Zhan, M., Hu, M.C., 2015. Klotho, stem cells, and aging. Clin. Interv. Aging. 10, 1233–1243.
Bloch, L., Sineshchekova, O., Reichenbach, D., Reiss, K., Saftig, P., Kuro-, o.M., Kaether, C., 2009. Klotho is a substrate for alpha-, beta- and gamma-secretase. FEBS. Lett. 583, 3221–3224.
Cai, Z., Zhao, B., Li, K., Zhang, L., Li, C., Quazi, S.H., Tan, Y., 2012. Mammalian target of rapamycin: a valid therapeutic target through the autophagy pathway for Alzheimer's disease? J. Neurosci. Res. 90, 1105–1118.
Cararo-Lopes, M.M., Mazucanti, C.H.Y., Scavone, C., Kawamoto, E.M., Berwick, D.C., 2017. The relevance of alpha-KLOTHO to the central nervous system: some key questions. Ageing. Res. Rev. 36, 137–148.
Chen, C.D., Podvin, S., Gillespie, E., Leeman, S.E., Abraham, C.R., 2007. Insulin stimulates the cleavage and release of the extracellular domain of Klotho by ADAM10 and ADAM17. Proc. Natl. Acad. Sci. U S A 104, 19796–19801.
Chen, C.D., Sloane, J.A., Li, H., Aytan, N., Giannaris, E.L., Zeldich, E., Hinman, J.D., Dedeoglu, A., Rosene, D.L., Bansal, R., Luebke, J.I., Kuro-, o.M., Abraham, C.R., 2013. The antiaging protein Klotho enhances oligodendrocyte maturation and myelination of the CNS. J. Neurosci. 33, 1927–1939.
Chen, C.D., Li, H., Liang, J., Hixson, K., Zeldich, E., Abraham, C.R., 2015. The anti-aging and tumor suppressor protein Klotho enhances differentiation of a human oligodendrocytic hybrid cell line. J. Mol. Neurosci. 55, 76–90.
Cho, M.H., Cho, K., Kang, H.J., Jeon, E.Y., Kim, H.S., Kwon, H.J., Kim, H.M., Kim, D.H., Yoon, S.Y., 2014. Autophagy in microglia degrades extracellular beta-amyloid fibrils and regulates the NLRP3 inflammasome. Autophagy 10, 1761–1775.
Cummings, J., Lee, G., Ritter, A., Zhong, K., 2018. Alzheimer's disease drug development pipeline: 2018. Alzheimers. Dement. 4, 195–214.
Dowson, J.H., Mountjoy, C.Q., Cairns, M.R., Wilton-Cox, H., 1992. Changes in intraneuronal lipopigment in Alzheimer's disease. Neurobiol. Aging. 13, 493–500.
Dowson, J.H., Mountjoy, C.Q., Cairns, M.R., Wilton-Cox, H., 1995. Alzheimer's disease: distribution of changes in intraneuronal lipopigment in the frontal cortex. Dementia 6, 334–342.
Dubal, D.B., Zhu, L., Sanchez, P.E., Worden, K., Broestl, L., Johnson, E., Ho, K., Yu, G.Q., Kim, D., Betourne, A., Kuro-, O.M., Masliah, E., Abraham, C.R., Mucke, L., 2015. Life extension factor klotho prevents mortality and enhances cognition in hAPP transgenic mice. J. Neurosci. 35, 2358–2371.
Goedert, M., 1987. Neuronal localization of amyloid beta protein precursor mRNA in normal human brain and in Alzheimer's disease. EMBO. J. 6, 3627–3632.
Gold, M., El Khoury, J., 2015. β-amyloid, microglia, and the inflammasome in Alzheimer's disease. Semin. Immunopathol. 37, 607–611.
Hardy, J.A., Higgins, G., 1992. Alzheimer's disease: the amyloid cascade hypothesis. Science 256, 184–185.
Hohn, A., Grune, T., 2013. Lipofuscin: formation, effects and role of macroautophagy. Redox. Biol. 1, 140–144.
Jankowsky, J.L., Fadale, D.J., Anderson, J., Xu, G.M., Gonzales, V., Jenkins, N.A., Copeland, N.G., Lee, M.K., Younkin, L.H., Wagner, S.L., Younkin, S.G.,

Borchelt, D.R., 2004. Mutant presenilins specifically elevate the levels of the 42 residue β-amyloid peptide in vivo: evidence for augmentation of a 42-specific γ secretase. Hum. Mol. Genet. 13, 159–170.
Jiang, T., Yu, J.T., Zhu, X.C., Tan, M.S., Wang, H.F., Cao, L., Zhang, Q.Q., Shi, J.Q., Gao, L., Qin, H., Yang, Y.D., Tan, L., 2014. Temsirolimus promotes autophagic clearance of amyloid-beta and provides protective effects in cellular and animal models of Alzheimer's disease. Pharmacol. Res. 81, 54–63.
Jiao, S.S., Yao, X.Q., Liu, Y.H., Wang, Q.H., Zeng, F., Lu, J.J., Liu, J., Zhu, C., Shen, L.L., Liu, C.H., Wang, Y.R., Zeng, G.H., Parikh, A., Chen, J., Liang, C.R., Xiang, Y., Bu, X.L., Deng, J., Li, J., Xu, J., Zeng, Y.Q., Xu, X., Xu, H.W., Zhong, J.H., Zhou, H.D., Zhou, X.F., Wang, Y.J., 2015. Edaravone alleviates Alzheimer's disease-type pathologies and cognitive deficits. Proc. Natl. Acad. Sci. U S A 112, 5225–5230.
Kalaria, R.N., Maestre, G.E., Arizaga, R., Friedland, R.P., Galasko, D., Hall, K., Luchsinger, J.A., Ogunniyi, A., Perry, E.K., Potocnik, F., Prince, M., Stewart, R., Wimo, A., Zhang, Z.X., Antuono, P., 2008. Alzheimer's disease and vascular dementia in developing countries: prevalence, management, and risk factors. Lancet. Neurol. 7, 812–826.
Kuang, X., Chen, Y.S., Wang, L.F., Li, Y.J., Liu, K., Zhang, M.X., Li, L.J., Chen, C., He, Q., Wang, Y., Du, J.R., 2014. Klotho upregulation contributes to the neuroprotection of ligustilide in an Alzheimer's disease mouse model. Neurobiol. Aging. 35, 169–178.
Kuang, X., Zhou, H.J., Thorne, A.H., Chen, X.N., Li, L.J., Du, J.R., 2017. Neuroprotective effect of ligustilide through induction of alpha-secretase processing of both APP and klotho in a mouse model of Alzheimer's disease. Front. Aging. Neurosci. 9, 353.
Kuro-o, M., Matsumura, Y., Aizawa, H., Kawaguchi, H., Suga, T., Utsugi, T., Ohyama, Y., Kurabayashi, M., Kaname, T., Kume, E., Iwasaki, H., Iida, A., Shiraki-Iida, T., Nishikawa, S., Nagai, R., Nabeshima, Y.I., 1997. Mutation of the mouse klotho gene leads to a syndrome resembling ageing. Nature 390, 45–51.
Kurosu, H., Yamamoto, M., Clark, J.D., Pastor, J.V., Nandi, A., Gurnani, P., McGuinness, O.P., Chikuda, H., Yamaguchi, M., Kawaguchi, H., Shimomura, I., Takayama, Y., Herz, J., Kahn, C.R., Rosenblatt, K.P., Kuro-, o.M., 2005. Suppression of aging in mice by the hormone Klotho. Science 309, 1829–1833.
Lee, J.K., Jin, H.K., Park, M.H., Kim, B.R., Lee, P.H., Nakauchi, H., Carter, J.E., He, X., Schuchman, E.H., Bae, J.S., 2014. Acid sphingomyelinase modulates the autophagic process by controlling lysosomal biogenesis in Alzheimer's disease. J. Exp. Med. 211, 1551–1570.
Li, C., Siragy, H.M., 2015. (Pro)renin receptor regulates autophagy and apoptosis in podocytes exposed to high glucose. Am. J. Physiol. Endocrinol. Metab. 309, 302–310.
Mandrekar-Colucci, S., Landreth, G.E., 2010. Microglia and inflammation in Alzheimer's disease. CNS. Neurol. Disord. Drug. Targets. 9, 156–167.
Masso, A., Sánchez, A., Bosch, A., Giménez-Llort, L., Chillón, M., 2017. Secreted alphaKlotho isoform protects against age-dependent memory deficits. Mol. Psychiatry. 23, 1–11.
Masso, A., Sánchez A, Gimenez-Llort L., Lizcano, J.M., Cañete, M., García, B., Torres-Lista, V., Puig, M., Bosch, A., Chillon, M., 2015. Secreted and transmembrane alphaKlotho isoforms have different spatio-temporal profiles in the brain during aging and Alzheimer's disease progression. PloS One 10, e0143623.
Mawuenyega, K.G., Sigurdson, W., Ovod, V., Munsell, L., Kasten, T., Morris, J.C., Yarasheski, K.E., Bateman, R.J., 2010. Decreased clearance of CNS beta-amyloid in Alzheimer's disease. Science 330, 1774.
Mayeux, R., Stern, Y., 2012. Epidemiology of Alzheimer disease. Cold. Spring. Harb. Perspect. Med. 2, a006239.
Murphy, M.P., LeVine, H., 2010. Alzheimer's disease and the β-amyloid peptide. J. Alzheimers. Dis. 19, 311–323.
Preston, S.D., Steart, P.V., Wilkinson, A., Nicoll, J.A., Weller, R.O., 2003. Capillary and arterial cerebral amyloid angiopathy in Alzheimer's disease: defining the perivascular route for the elimination of amyloid β from the human brain. Neuropathol. Appl. Neurobiol. 29, 106–117.
Reiserer, R.S., Harrison, F.E., Syverud, D.C., McDonald, M.P., 2007. Impaired spatial learning in the APPSwe + PSEN1DeltaE9 bigenic mouse model of Alzheimer's disease. Genes. Brain. Behav. 6, 54–65.
Roberts, K.F., Elbert, D.L., Kasten, T.P., Patterson, B.W., Sigurdson, W.C., Connors, R.E., Ovod, V., Munsell, L.Y., Mawuenyega, K.G., Miller-Thomas, M.M., Moran, C.J., Cross 3rd, D.T., Derdeyn, C.P., Bateman, R.J., 2014. Amyloid-beta efflux from the central nervous system into the plasma. Ann. Neurol. 76, 837–844.
Sagare, A.P., Bell, R.D., Zhao, Z., Ma, Q., Winkler, E.A., Ramanathan, A., Zlokovic, B.V., 2013. Pericyte loss influences Alzheimer-like neurodegeneration in mice. Nat. Commun. 4, 2932.
Semba, R.D., Moghekar, A.R., Hu, J., Sun, K., Turner, R., Ferrucci, L., O'Brien, R., 2014. Klotho in the cerebrospinal fluid of adults with and without Alzheimer's disease. Neurosci. Lett. 558, 37–40.
Terman, A., Brunk, U.T., 1998. Lipofuscin: mechanisms of formation and increase with age. APMIS 106, 265–276.
Tian, Y., Bustos, V., Flajolet, M., Greengard, P., 2011. A small-molecule enhancer of autophagy decreases levels of Abeta and APP-CTF via Atg5-dependent autophagy pathway. FASEB. J. 25, 1934–1942.
Viswanathan, A., Greenberg, S.M., 2011. Cerebral amyloid angiopathy in the elderly. Ann. Neurol. 70, 871–880.
Wang, H.C., Zhang, T., Kuerban, B., Jin, Y.L., Le, W., Hara, H., Fan, D.S., Wang, Y.J., Tabira, T., Chui, D.H., 2015. Autophagy is involved in oral rAAV/Abeta vaccine-induced Abeta clearance in APP/PS1 transgenic mice. Neurosci. Bull. 31, 491–504.
Wang, Y.J., Zhou, H.D., Zhou, X.F., 2006. Clearance of amyloid-beta in Alzheimer's disease: progress, problems and perspectives. Drug. Discov. Today. 11, 931–938.
Wolfe, D.M., Lee, J.H., Kumar, A., Lee, S., Orenstein, S.J., Nixon, R.A., 2013. Autophagy failure in Alzheimer's disease and the role of defective lysosomal acidification. Eur. J. Neurosci. 37, 1949–1961.
Wu, N., Rao, X., Gao, Y., Wang, J., Xu, F., 2013. Amyloid-beta deposition and olfactory dysfunction in an Alzheimer's disease model. J. Alzheimers. Dis. 37, 699–712.
Yao, Y., Tsirka, S.E., 2011. Truncation of monocyte chemoattractant protein 1 by plasmin promotes blood–brain barrier disruption. J. Cell. Sci. 124 (Pt 9), 1486–1495.
Zeldich, E., Chen, C.D., Colvin, T.A., Bove-Fenderson, E.A., Liang, J., Tucker Zhou, T.B., Harris, D.A., Abraham, C.R., 2014. The neuroprotective effect of Klotho is mediated via regulation of members of the redox system. J. Biol. Chem. 289, 24700–24715.
Zhou, H.J., Li, H., Shi, M.Q., Mao, X.N., Liu, D.L., Chang, Y.R., Gan, Y.M., Kuang, X., Du, J.R., 2017. Protective effect of klotho against ischemic brain injury is associated with inhibition of RIG-I/NF-kappaB signaling. Front. Pharmacol. 8, 950.
Zhou, H.J., Zeng, C.Y., Yang, T.T., Long, F.Y., Kuang, X., Du, J.R., 2018. Lentivirus-mediated klotho up-regulation improves aging-related memory deficits and oxidative stress in senescence-accelerated mouse prone-8 mice. Life. Sci. 200, 56–62.